

# Entanglement spectrum of correlated electron states

Archak Purkayastha<sup>1,2,\*</sup> and V. Subrahmanyam<sup>2,†</sup>

<sup>1</sup>*International Centre for Theoretical Sciences, Tata Institute of Fundamental Research, Bangalore-560012, India*

<sup>2</sup>*Department of Physics, Indian Institute of Technology, Kanpur-208 016, India*

(Dated: May 15, 2022)

Entanglement spectrum of finite-size correlated electron systems are investigated using the Gutzwiller projection technique. The product of largest eigenvalue and rank of the block reduced density matrix is seen to characterise the insulator to metal crossover in the state. The fraction of distinct eigenvalues exhibits a ‘chaotic’ behaviour in the crossover region, and it shows a ‘integrable’ behaviour at both insulating and metallic ends. The block entanglement spectrum obeys conformal field theory (CFT) prediction at the metal and insulator ends, but the entanglement spectrum shows a noticeable deviation from CFT prediction in the crossover regime, thus it can also track a metal-insulator transition. A modification of the CFT result for the entanglement spectrum for finite size is proposed which holds in the crossover regime also. The adjacent level spacing distribution of unfolded non-zero eigenvalues for intermediate values of Gutzwiller projection parameter  $g$  is the same as that of an ensemble of random matrices obtained by replacing each block of reduced density matrix by a random real symmetric Toeplitz matrix. It is strongly peaked at zero, with an exponential tail proportional to  $e^{-(n/R)^s}$ , where  $s$  is the adjacent level spacing,  $n$  is number of distinct eigenvalues and  $R$  is the rank of the reduced density matrix.

PACS: 03.67.Mn, 05.45.Mt, 71.30.+h, 71.27.+a

Quantum entanglement of a system quantifies the correlations between the parts of the system[1], which serves as a resource for quantum information processing tasks. The block entanglement, viz. the entropy of a subsystem, is a widely-used entanglement measure, that has been used to investigate critical behaviour near quantum phase transitions in spin systems[2, 3]. But there are not many studies of the entanglement in interacting electron systems, which exhibit substantially richer structure than interacting spin systems as they carry additional charge degrees of freedom. In this article, we study the strong correlation effect on the entanglement spectrum of the one-dimensional Gutzwiller state[4], as a proto-type strongly-correlated state. In this state, the strong on-site correlation effect of the Hubbard model ground state is mimicked by applying a projection operator on the non-interacting metallic state to decrease the double occupancy. At one end of the control parameter is the metallic state with no projection, viz. a Fermi ground state constructed from occupying lowest-lying one-electron plane-wave states for both up and down spin electrons. The metallic state maximises the double occupancy as there is no correlation between the up and down spin electron. At the other extreme, there is an insulator phase, corresponding to the fully-projected state with no double occupancy. The Gutzwiller state for a lattice of  $N$  sites is given by

$$|g\rangle = \prod_{i=1}^N \{1 - (1-g)\hat{n}_{i\uparrow}\hat{n}_{i\downarrow}\}|F\rangle, \quad (1)$$

where  $|F\rangle = \prod_{k=0}^{k_F} \hat{c}_{k\uparrow}^\dagger \hat{c}_{k\downarrow}^\dagger |0\rangle$  is the metallic Fermi state constructed from the vacuum state by using electron creation operators  $\hat{c}_{k\sigma}^\dagger$  with a momentum  $k$  and spin  $\sigma$ , and  $g$  is a parameter taking values from 0 to 1,  $g = 1$  being the non-interacting case, and  $g = 0$  being the limit of infinite interactions. The filling factor is determined by  $k_F$ , the Fermi momentum. We consider a ring with  $N$  electrons, with equal number of up and down spins, corresponding to the half-filling case. We partition the system into two equal parts, with the first  $N/2$  sites belong to one subsystem.

The block entanglement entropy of the Gutzwiller state for half bipartition has been studied[6] as a function of the correlation factor and the number of sites. At the two ends, viz. for the metallic state at  $g = 1$  and the insulating state at  $g = 0$ , even for small size systems, it shows a logarithmic increase as a function  $N$ , as predicted by conformal field theory (CFT)[7]. For intermediate values of  $g$ , the finite size corrected central charge is shown to obey a scaling form, with a metal-insulator crossover predicted for  $N^{1/3}g \approx 0.24$ ,  $N < 10^5$ . The metal-insulator crossover is driven by the fact that, for intermediate values of  $g$ , even though the correlation length between same kind of spins remains infinite, the correlation length between opposite spins becomes finite and decreases with  $g$ . For  $g = 1$ , this correlation length is zero so system becomes scale invariant again. Hence, for intermediate values of  $g$ , there are two relevant length scales : the system size and the correlation length between opposite spins. The physics is governed by the ratio of these two length scales and the insulator to metal crossover occurs when these two are equal. Further, the entanglement entropy has been shown to be related to the number and spin fluctuations of the block, and is determined by the jump at the fermi surface. These results

\*Electronic address: archakp@icts.res.in

†Electronic address: vmani@iitk.ac.in

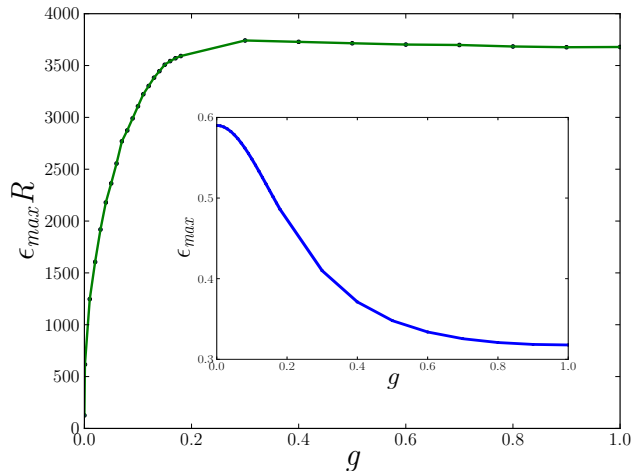


FIG. 1: The variation of the product of the largest eigenvalue  $\epsilon_{max}$  and rank  $R$  of the reduced density matrix with on-site correlation factor  $g$  for  $N = 16$  sites at half-filling is shown. The inset shows the variation of  $\epsilon_{max}$  with  $g$ . Crossover to metallic limit is shown by the product becoming almost constant.

for the metal-insulator crossover point seem to compare well with an experiment on Ni nano-chains. In this paper, we will investigate the spectral features of the block reduced density matrix for half bipartition. The results are based on exact numerical Schmidt decomposition of systems upto  $N = 16$  sites.

The distribution of eigenvalues of the reduced density matrix, known as the entanglement spectrum [8], is supposed to carry more information than entanglement entropy and it may provide a deeper understanding of the quantum correlations of the system. Calabrese and Lefevre gave an expression for entanglement spectrum of gapless one dimensional spin systems via CFT calculations [7]. It will be interesting to see if a similar result is valid for finite size correlated electron systems.

The dimension of the reduced density matrix of the subsystem with  $N/2$  sites is  $2^N$ , and in principle as many eigenvalues can be nonzero. However, the entanglement entropy shows only a logarithmic divergence with  $N$ , implying only  $O(N)$  number of nonzero eigenvalues. Thus the rank of the reduced density matrix is vastly reduced. Since on-site correlation factor  $g$  reduces the probability of doubly-occupied sites, the rank is reduced as  $g$  decreases. Reduction of the rank of the reduced density matrix is one of the reasons for a decrease of the entanglement as  $g \rightarrow 0$ .

For reduced density matrix of a given rank  $R$ , entanglement entropy is maximum when all the eigenvalues are equal. Thus, in this case, each eigenvalue is equal to  $1/R$ . This then is the optimal eigenvalue. But, we find for the Gutzwiller state, most of the eigenvalues are very close to zero. In fact, about 98% of eigenvalues are less than  $1/R$

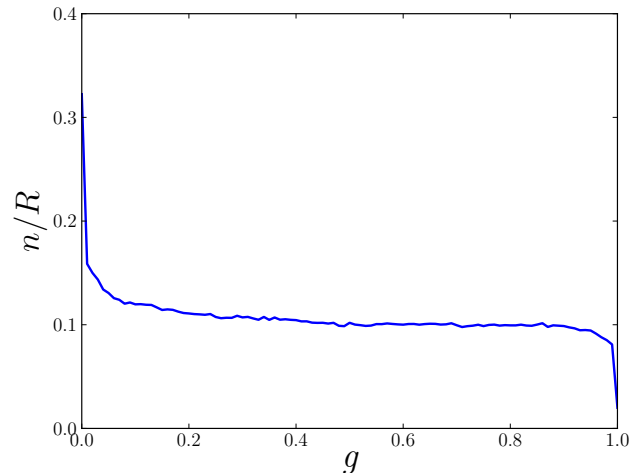


FIG. 2: Variation of ratio of number of distinct eigenvalues  $n$  to rank  $R$  with  $g$  for  $N = 16$  sites at half-filling is shown. It remains nearly constant, exhibiting a ‘chaotic’ behaviour in the crossover region, but it decreases with  $g$  close to  $g = 0$  and  $g = 1$ , showing an ‘integrable’ behavior.

for the non-interacting case. The number reduces only to about 96% for the strongly-interacting case. But, interestingly, we find that the remaining 2 to 4 per cent eigenvalues greater than  $\frac{1}{R}$  determine the entanglement entropy correct to two significant figures in all cases.

The largest eigenvalue is an important parameter governing the distribution of eigenvalues. The range of the distribution of eigenvalues  $\{\epsilon_i\}$  is determined by the largest eigenvalue  $\epsilon_{max}$ . For Gutzwiller state at half-filling,  $\epsilon_{max}$  decreases as correlation factor  $g$  increases. This is because, as the rank of the reduced density matrix increases, the normalisation factor demands a decrease of  $\epsilon_{max}$ . We argue that, in such a case, the variation of the product  $\epsilon_{max} R$ , which is just the ratio of the maximum eigenvalue  $\epsilon_{max}$  to the optimal eigenvalue  $1/R$ , should capture the essential physics of the state. In Fig.1, we see that the product  $\epsilon_{max} R$  increases rapidly from the insulating limit and saturates at the metallic limit at  $g = 1$ . The onset of the crossover to metallic region is seen by the product becoming almost constant. The crossover region shown by this curve matches with that from the scaling form for the entanglement entropy[6].

The nonzero eigenvalues of the reduced density matrix are highly degenerate. Both the rank of the reduced density matrix and the degeneracy of eigenvalues increase with  $g$ , causing the number of distinct eigenvalues to vary in a nonmonotonically with  $g$ . An interesting quantity to study is the ratio of the number of distinct eigenvalues  $n$  to the rank  $R$ . This study is commonly undertaken for energy eigenvalues of integrable and chaotic systems. In the integrable regime, which is associated with degeneracies growing with size and energy, the ratio decreases

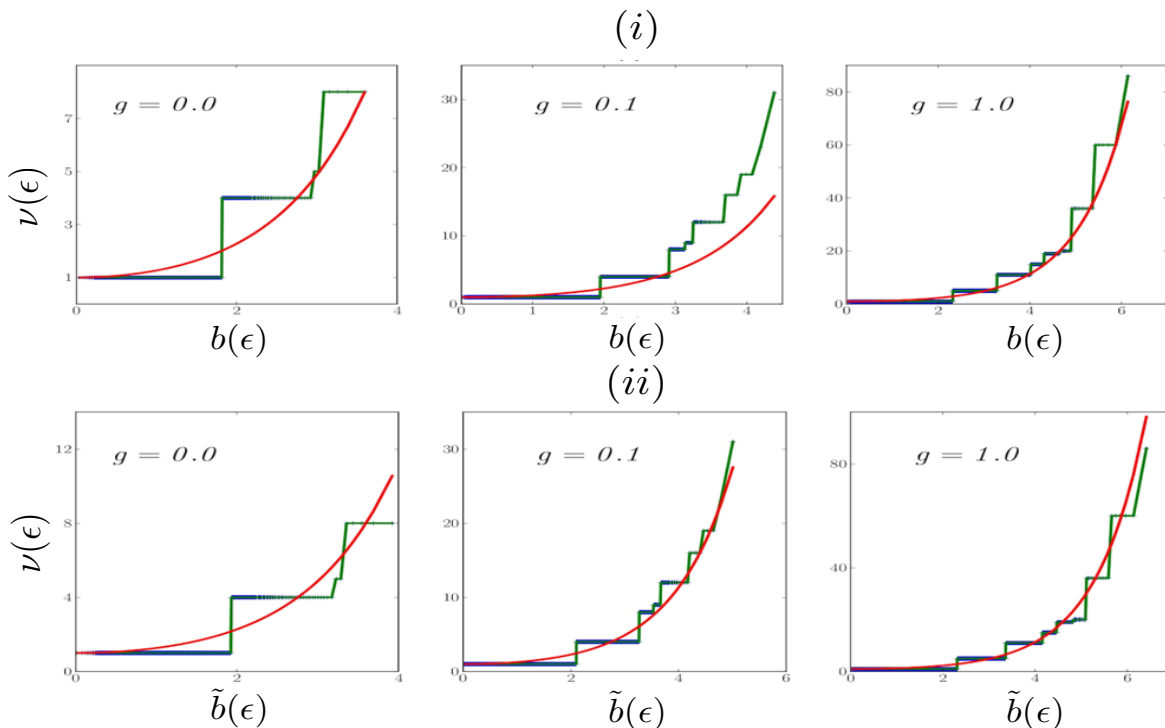


FIG. 3: The staircase plots show the integrated density of eigenvalues  $\nu(\epsilon)$  for  $N = 16$  sites at half filling for various  $g$  values (i) with  $b(\epsilon) = 2\sqrt{\ln(\epsilon_{max})\ln(\frac{\epsilon}{\epsilon_{max}})}$ , along with the corresponding CFT (smooth curve) result given in Eq.4,(ii) with  $\tilde{b}(\epsilon) = 2\sqrt{|\frac{S}{2}(\ln \epsilon + \frac{S}{2})|}$ , along with the modified CFT (smooth curve) result given in Eq.7.  $g = 0.0$  corresponds to the insulating state,  $g = 0.1$  ( $\simeq 0.24/N^{\frac{1}{3}}$ ) corresponds to the crossover,  $g = 1.0$  corresponds to the metallic state.

with energy. In the chaotic regime, degeneracies being rare, the ratio remains nearly constant. Fig 2 shows the variation of this ratio with  $g$  for the eigenvalues of the reduced density matrix of half-filled Gutzwiller state. We see that  $n/R$  remains nearly constant, exhibiting a ‘chaotic’ behaviour in the metal-insulator crossover region, but it decreases with  $g$  close to  $g = 0$  (insulating end) and  $g = 1$  (metallic end), showing an ‘integrable’ behavior. Following the scaling theory of entanglement entropy[6], the correct scaling variable is a product of an increasing function of  $g$  and an increasing function of  $N$ . Thus, the variation with  $g$  for fixed  $N$  is representative of variation with  $N$  for fixed  $g$ .

Next we look at the density distribution of non-zero eigenvalues. The block entanglement entropy can be written, using the density of eigenvalues, as

$$\begin{aligned}
 S &= - \sum_i \epsilon_i \ln \epsilon_i \\
 &= \int_0^1 d\epsilon (1 + \ln \epsilon) (R - \nu(\epsilon))
 \end{aligned}
 \tag{2}$$

Here, the integrated density of eigenvalues  $\nu(\epsilon)$  is given by

$$\nu(\epsilon) = \sum_i \Theta(\epsilon_i - \epsilon).
 \tag{3}$$

Calabrese and Lefevre[7] calculated this function for one-dimensional gapless systems, and it is given by

$$\nu(\epsilon) = I_0(2\sqrt{-b_0 \ln(\frac{\epsilon}{\epsilon_{max}})})
 \tag{4}$$

where  $I_0$  is modified Bessel function of zeroth order,  $\epsilon_{max}$  is the largest eigenvalue, and

$$b_0 = \frac{c}{6} \ln N \simeq -\ln \epsilon_{max}
 \tag{5}$$

Here  $c$  is central charge of the underlying CFT. The entanglement entropy of gapless 1D spin systems diverge logarithmically and  $c$  turns out to be the coefficient of the logarithmic term. Entanglement entropy  $S$  comes out to be :

$$S \simeq -2 \ln \epsilon_{max}
 \tag{6}$$

Their result is universally valid whenever the system can be described by a CFT. The entanglement entropy of the Gutzwiller state is shown to follow the CFT results at the metallic and insulating limits even for finite size, and deviates in the crossover region[6]. Thus, the metal-insulator crossover can be tracked from the deviation of the entanglement spectrum from the above CFT result.

In Fig.3, the integrated eigenvalue density the  $\nu$  is plotted as a function of  $b = 2\sqrt{\ln(\epsilon_{max})\ln(\frac{\epsilon}{\epsilon_{max}})}$  for  $N = 16$  sites for various values of on-site correlation factor  $g$ , along with the corresponding plots of the CFT result given above. The crossover is marked by a deviation from the CFT result.

The CFT formalism describes the entanglement spectrum in terms of one parameter, which in the above case, is the largest eigenvalue  $\epsilon_{max}$ . We generalize Eq. 4 by recasting it in terms of the entanglement entropy  $S$ ,

$$\nu(\epsilon) \simeq I_0(2\sqrt{|b_0(\ln \epsilon + b_0)|}), \quad (7)$$

where  $b_0$  is given by (generalizing Eq. 5),

$$b_0 = \frac{S}{2} \quad (8)$$

We have shown in Fig.3 the entanglement spectrum staircase plotted with the modified function given above. It is seen that Eq.7 holds approximately for all values of  $g$ . This equation of course gives back Eq.4 for large  $N$ . The reason this equation works for all values of  $g$  while Eq.4 holds only for  $g = 0$  and  $g = 1$  goes back to the observation that for intermediate values of  $g$  there are two length scales in the system [6]. The largest eigenvalue does not capture the full information about both the length scales, whereas the entanglement entropy have the information about both the length scales. Hence, when the equation is recast in terms of entanglement entropy, it holds for all values of  $g$ . At  $g = 0$  and  $g = 1$ , there is only one length scale, viz. the system size, and Eq.4 holds.

Spacing distribution of eigenvalues of Hamiltonian systems has been traditionally used to investigate the quantum chaos[9], and to track metal-insulator transition[10]. The uncorrelated metallic state shows a ‘correlated’ single-particle energy level spacing distribution with level repulsion, whereas the correlated insulator state is associated with a ‘uncorrelated’ Poisson spacing distribution. For a chaotic system, the spacing distribution is seen to be same as that of an ensemble of random matrices having the same number of degrees of freedom as the system. From our investigation of fraction of distinct eigenvalues we have found that for crossover values of  $g$ , the eigenvalues of reduced density matrix behave like a ‘chaotic’ system. So, in this region, we expect that the spacing distribution of eigenvalues of  $\rho_A$  can be understood from a random matrix ensemble.

For that purpose, we first look at the symmetries of  $\rho_A$ .  $\rho_A$  is block diagonal, with each block specified by the number of up spins  $N_{A\uparrow}$  and the number of down spins  $N_{A\downarrow}$  in  $A$ . Furthermore, we note that the labels of

$\uparrow$  and  $\downarrow$ , as well as those of  $A$  and  $B$  are arbitrary and can be interchanged. Hence the eigenvalues of blocks of reduced density matrix with spins flipped are same. Also, all the eigenvalues from blocks with  $N_A$  particles in  $A$  are same as those from blocks with  $N - N_A$  particles in  $A$ .

Finding eigenvalues of each block of  $\rho_A$  is a formidable task because the size and number of blocks increase exponentially with  $N$ . Let  $R$  denote a block of the reduced density matrix  $\rho_A$  with  $N_{A\uparrow} = p$  and  $N_{A\downarrow} = q$ . The matrix element  $R_{ij}$  between two configurations labeled by the set of positions of up and down spin electrons in subsystem  $A$  is given by,

$$R_{ij} = Q f_{ij}^A(g) \sum_{b_\uparrow, b_\downarrow} f_{b_\uparrow b_\downarrow}^B(g) \times D_k(i_{a\uparrow}, b_\uparrow) D_k(i_{a\downarrow}, b_\downarrow) D_k^*(j_{a\uparrow}, b_\uparrow) D_k^*(j_{a\downarrow}, b_\downarrow), \quad (9)$$

where  $Q$  is constant that depends on  $N$ ,  $N_{A\uparrow}$  and  $N_{A\downarrow}$ ,  $f_{ij}^A(g)$  is a function of  $g$  coming from the double occupancy of the configurations  $i$  and  $j$  of subsystem  $A$ ,  $f_{b_\uparrow b_\downarrow}^B(g)$  is a function  $g$  coming from the double occupancy of the configuration of subsystem  $B$ . The label  $i_{a\uparrow}$  ( $i_{a\downarrow}$ ) is a set of  $p$  ( $q$ ) numbers giving positions of up (down) spins in subsystem  $A$  in  $i$ th configuration and similarly for the  $j$ th configuration, and  $b_\uparrow$  ( $b_\downarrow$ ) is the set of positions of up (down) spin in subsystem  $B$ , and  $D_k(r)$  is the Slater determinant with momentum labels given by the set  $k$  and position labels given by the set  $r$ ,  $*$  denotes complex conjugate. The sum is over all possible configurations of  $B$ , i.e, all possible choices of  $b_\uparrow$  and  $b_\downarrow$ . Writing out the Slater determinants explicitly and simplifying, it can be shown that there are some terms in the sum that are independent of the configurations of  $B$ . Upon performing the sum over configurations of  $B$ , these terms add up coherently whereas the other terms add incoherently. Since the number of all possible configurations of  $B$  is quite large, we can approximate  $R_{ij}$  by considering only the terms independent of configurations of  $B$ . These terms will only pick up a factor of some constant times a function of  $g$  from the sum. The result is of the form :

$$R_{ij} \simeq Q f_{ij}(g) \left[ \sum_{k_p} D_{k_p}(i_{a\uparrow}) D_{k_p}^*(j_{a\uparrow}) \sum_{k_q} D_{k_q}(i_{a\downarrow}) D_{k_q}^*(j_{a\downarrow}) \right] \equiv Q f_{ij} M_{ij}, \quad (10)$$

where all constants have been absorbed into  $Q$ , all  $g$  dependence coming from both subsystems  $A$  and  $B$  has been absorbed into  $f_{ij}(g)$ ,  $k_p$  ( $k_q$ ) is a set of  $p$  ( $q$ ) values of  $k$  chosen from all possible values of  $k$  below  $k_F$  and the sums are over all possible such choices,  $M_{ij}$  is the term within square brackets which is the sum of all possible terms in Eq 9 which are independent of configurations of  $B$ . Since taking complex conjugate of Slater determinant simply means  $k \rightarrow -k$ , and since both these levels are allowed, the above sums are real. Thus the  $M_{ij}$  is real. Also due to the same reason,  $M_{ij}$  depends only on the relative positions of up (down) spins in the

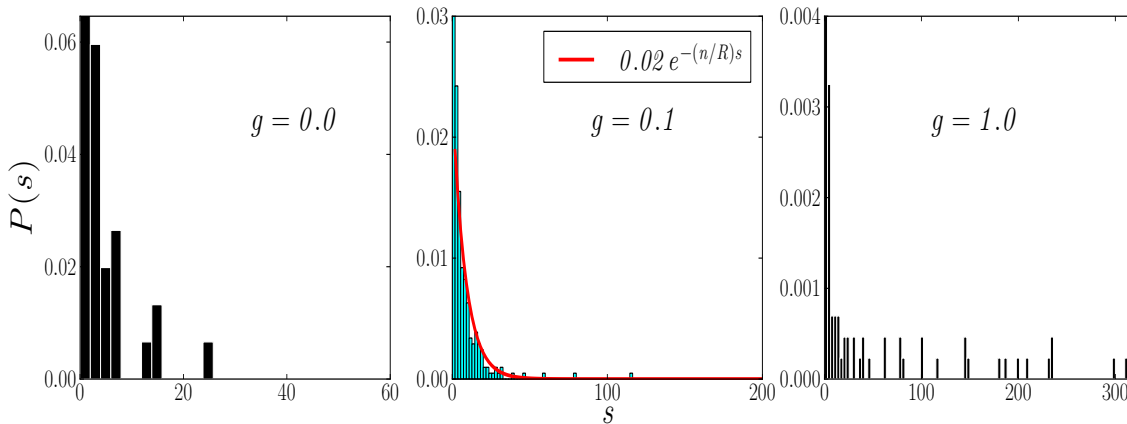


FIG. 4: Spacing distribution of the unfolded eigenvalues of  $\rho_A$  is plotted with the adjacent level spacing  $s$ , for  $N = 16$  sites at half-filling for various values of  $g$ . The height of the big peak at  $s = 0$  for all  $g$  is not shown in the figure as it would wash out the structure at other values of  $s$ . At intermediate values of  $g$ , where the system is ‘chaotic’, the tail of the distribution decays exponentially as  $e^{-(n/R)s}$  where  $n$  is the number of distinct eigenvalues and  $R$  is the rank of  $\rho_A$ . This is as expected from random matrix theory. The spacing distribution at the two ends  $g = 0$  and  $g = 1$  has a different nature because the system is ‘integrable’ at those values of  $g$ .

$i$ th and  $j$ th configurations. These properties manifest in symmetries of the matrix  $M$ . For  $N = 4$ , explicit calculation shows that the matrix  $M$  is a real symmetric Toeplitz matrix. For example, for  $N = 4$ , for the block with  $N_{A\uparrow} = 1$  and  $N_{A\downarrow} = 1$ ,  $M_{ij}$  is given by :

$$M_{ij} = 1 + \cos \frac{\pi}{2} (i_{a\uparrow} - j_{a\uparrow}) + \cos \frac{\pi}{2} (i_{a\downarrow} - j_{a\downarrow}) + \cos \frac{\pi}{2} (i_{a\uparrow} - j_{a\uparrow} + i_{a\downarrow} - j_{a\downarrow}) \quad (11)$$

which can be cast into Toeplitz form with proper ordering. For  $N = 6$ , the matrix  $M$  becomes block real symmetric Toeplitz matrix with each block also being a real symmetric Toeplitz matrix. Such a matrix has the same number of degrees of freedom as a real symmetric Toeplitz matrix. However, it is difficult to prove such a result for general  $N$ .

The projection factor  $f_{ij}(g)$  makes further analytical calculation difficult even for  $N = 6$ . However, since we know the system is ‘chaotic’ for crossover values of  $g$  and since  $M$  has same number of degrees of freedom as a real symmetric Toeplitz matrix, we claim that the adjacent level spacing distribution will be the same as that of an ensemble of random matrices obtained by replacing each block of  $\rho_A$  by a random real symmetric Toeplitz matrix whose elements are drawn from some distribution with mean 0 and variance 1. Ensemble of such random real symmetric Toeplitz matrices have been previously investigated and the spacing distribution is found to be Poisson distribution, and not the usual GOE spacing distribution [11]. This is because the number of degrees of freedom of  $\tilde{N} \times \tilde{N}$  real symmetric Toeplitz matrix is  $2\tilde{N} - 1$  and not  $O(\tilde{N}^2)$ . In our case, since sizes of blocks vary, we have many ensembles of random real symmetric Toeplitz matrices of various sizes. So the spacing distri-

bution will not exactly be the Poisson distribution. Since size of matrix is the only parameter in a random matrix ensemble, blocks of same size will have same distribution of eigenvalues. Also eigenvalue distributions of blocks of different sizes will overlap. Hence, probability of degeneracy of the eigenvalues will be very high. Thus in the spacing distribution, there will be a pronounced peak at zero spacing. Apart from the peak, the effect of having blocks of various sizes will be to slow down the Poisson like decay. So the exponent in Poisson distribution will pick up a constant factor. The amplitude of the Poisson like decay function will be much smaller than the peak at zero spacing. Thus the spacing distribution we expect from random matrix theory is highly peaked at zero and having an exponentially decaying tail, the peak being much higher than amplitude of the exponential function. The exponential decay scale depends, as we will see below (see Fig.4), on the ratio of the number of distinct eigenvalues and the rank that we have investigated (see Fig.2) earlier.

To check the above result with exact numerical calculations, we need to unfold the eigenvalue spectrum to get a non-trivial distribution, viz. the average spacing of the unfolded energy level should be independent of the system size. We define the unfolded eigenvalues  $\{\tilde{\epsilon}_i\}$ , using the analytical result of the spectrum given in Eq.7,

$$\tilde{\epsilon}_i = I_0 \left( 2 \sqrt{ \left| \frac{S}{2} (\ln \epsilon_i + \frac{S}{2}) \right| } \right) \quad (12)$$

The adjacent level spacing distribution is then given by,

$$P(s) = \sum_i \delta \left( s - \frac{|\tilde{\epsilon}_i - \tilde{\epsilon}_{i+1}|}{\Delta} \right). \quad (13)$$

where  $\Delta$  is the mean adjacent level spacing of  $\tilde{\epsilon}_i$ . Even

though the distribution of  $\epsilon_i$  is constrained by  $\sum_i \epsilon_i = 1$ , the above distribution is unconstrained because  $\tilde{\epsilon}_i$  diverges as  $\epsilon_i \rightarrow 0$ . This distribution is seen to be exactly as expected from our random matrix analysis. The constant factor in the exponent is phenomenologically found to be equal to the fraction of distinct eigenvalues  $n/R$ , which would of course be equal to 1 if there were no degeneracy. Furthermore, even though our analysis was for  $N = 4, 6$ , it is seen to hold for higher values of  $N$  also. This suggests that even for  $N > 6$ , the matrix  $M$  corresponding to a block of size  $\tilde{N}$  of  $\rho_A$  is a matrix with  $\tilde{N}$  degrees of freedom. The distribution for  $N = 16$  sites is shown in Fig.4 for various values of  $g$ . At  $g = 0$  and  $g = 1$ , the spacing distribution is different because there the system is ‘integrable’.

Away from the half-filling case, none of the above measures show much variation with the correlation factor  $g$ , which goes well with our results from calculation of entanglement entropy.

We have investigated eigenvalue spectrum of the reduced density matrix, as a function of the correlation factor  $g$  for Gutzwiller state at half-filling. We have found that the rank  $R$  and the largest eigenvalue  $\epsilon_{max}$  of the reduced density matrix vary in such a way that their prod-

uct clearly demarcates the insulating and metallic regions. In the insulating region it increases rapidly with  $g$  and becomes almost constant in the metallic region. The fraction of distinct eigenvalues  $n/R$  exhibits a ‘chaotic’ behaviour in the crossover region, and it shows a ‘integrable’ behaviour at both insulating and metallic ends.

We have shown that the deviation of the integrated entanglement spectrum from the CFT results can be used to track the metal-insulator crossover region. We have also proposed a modification of the CFT result for integrated entanglement spectrum which approximately holds over the entire range of  $g$ .

We have investigated the spacing distribution of non-zero eigenvalues of the reduced density matrix and have provided an understanding of it in terms of random matrices. The adjacent level spacing distribution of unfolded non-zero eigenvalues for intermediate values of Gutzwiller projection parameter  $g$  is the same as that of an ensemble of random matrices obtained by replacing each block of reduced density matrix by a random real symmetric Toeplitz matrix. It is strongly peaked at zero, with an exponential tail proportional to  $e^{-(n/R)s}$ , where  $s$  is the adjacent level spacing, the proportionality constant being much smaller than the height of the peak at zero spacing.

- 
- [1] M. A. Nielsen and I. L. Chuang, Quantum Computation and Quantum Information (Cambridge University Press, Cambridge, 2000).
  - [2] J. Eisert, M. Cramer, and M. B. Plenio, Rev. Mod. Phys., 82 (2010)
  - [3] S. Sahoo, V.M. Goli, S. Ramasesha, and D. Sen, J Phys Condens Matter 24, 115601 (2012)
  - [4] M. C. Gutzwiller, Phys. Rev. A137, 1726 (1965).
  - [5] W. Metzner and D. Vollhardt, Phys. Rev. B37, 7382 (1988).
  - [6] A. Purkayastha and V. Subrahmanyam, Phys. Rev. B. 89, 195125 (2014)
  - [7] P. Calabrese and A. Lefevre, Phys. Rev A 78, 032329 (2008)
  - [8] H. Li and F. D. M. Haldane, Phys. Rev. Lett. 101, 010504 (2008)
  - [9] O. Bohigas, M. J. Giannoni, and C. Schmit, Phys. Rev. Lett. 52, 1 (1984)
  - [10] B. I. Shklovskii, B. Shapiro, B. R. Sears, P. Lambrianides, and H. B. Shore, Phys. Rev. B47, 11487 (1993); I. Varga, E. Hofstetter, M. Schreiber, and J. Pipek, Phys. Rev. B 52, 7783 (1995)
  - [11] C. Hammond, S. J. Miller, Journal of Theoretical Probability, Vol. 18 (2005), no. 3, 537 - 566